Streptococcal Lancefield polysaccharides are critical cell wall determinants for human group IIA secreted phospholipase A2 to exert its bactericidal effects

Vincent P. van Hensbergen[1], Elin Movert[2], Vincent de Maat[1], Yoann Le Breton[4], Gérard Lambeau[5], Christine Payré[5], Anna Henningham[6,#], Victor Nizet[6, 7], Jos A.G. van Strijp[1], Fredric Carlsson[2, 3], Kevin S. McIver[4], Nina M. van Sorge[1] *

[1]Medical Microbiology, University Medical Center Utrecht, Utrecht, University, Utrecht, The Netherlands; [2]Department of Experimental Medical Science, Section for Immunology and [3]Department of Biology, Section for Molecular Cell Biology, Lund University, Lund, Sweden; [4]Department of Cell Biology & Molecular Genetics and Maryland Pathogen Research Institute, University of Maryland, College Park, Maryland, United States of America; [5]Université Côte d'Azur, CNRS, Institut de Pharmacologie Moléculaire et Cellulaire, Valbonne, France; [6]Department of Pediatrics and [7]Skaggs School of Pharmacy & Pharmaceutical Sciences, University of California, San Diego, La Jolla, CA, United States of America.

Child Healthy Research Centre, The University of Queensland, Brisbane, Australia; a.henningham@uq.edu.au

* Corresponding author: nsorge3@umcutrecht.nl

Short title

Bactericidal mechanism of hGIIA against streptococci

Abstract

Human Group IIA secreted phospholipase A_2 (hGIIA) is an acute phase protein with bactericidal activity against Gram-positive bacteria. Infection models in hGIIA transgenic mice have highlighted the importance of hGIIA as an innate defense mechanism against the human pathogens Group A *Streptococcus* (GAS) and Group B *Streptococcus* (GBS). Compared to other Gram-positive bacteria, GAS is remarkably resistant to hGIIA activity. To identify GAS resistance mechanisms, we exposed a highly saturated GAS M1 transposon library to recombinant human hGIIA and compared relative mutant abundance with library input through transposon-sequencing (Tn-seq). Based on transposon prevalence in the output library, we identified nine genes, including *dltA* and *lytR,* conferring increased hGIIA susceptibility. In addition, seven genes conferred increased hGIIA resistance, which included two genes, *gacH* and *gacI* that are located within the Group A Carbohydrate (GAC) gene cluster. Using GAS 5448 wild-type and the isogenic *gacI* mutant and gacI-complemented strains, we demonstrate that loss of the GAC *N*-acetylglucosamine (GlcNAc) side chain in the Δ*gacI* mutant increases hGIIA resistance approximately 10-fold, a phenotype that is conserved across different GAS serotypes. Increased resistance is associated with delayed penetration of hGIIA through the cell wall. Correspondingly, loss of the Lancefield Group B Carbohydrate (GBC) rendered GBS significantly more resistant to hGIIA-mediated killing. This suggests that the streptococcal Lancefield antigens, which are critical determinants for streptococcal physiology and virulence, are required for the human bactericidal enzyme hGIIA to exert its bactericidal function.

Author summary

The human immune system is capable of killing invading bacteria by secreting antimicrobial proteins. Cationic human Group IIA secreted phospholipase A_2 (hGIIA) is especially effective against Gram-positive bacteria by degrading the bacterial membrane. HGIIA requires binding to negatively charged surface structures before it can penetrate through the thick peptidoglycan layer and reach the target phospholipid membrane. Both binding and penetration are dependent on the cationic properties of hGIIA and anionic surface charge of bacteria. HGIIA is constitutively expressed at high concentrations at sites of possible bacterial entry, e.g. in tears, skin and small intestine. In serum, normal concentrations are low but can increase up to 1,000-fold upon inflammation or infection. HGIIA is important for defense against two human pathogens, Group A and Group B *Streptococcus* (GAS, GBS), as shown in mouse infection models. We demonstrate that the Lancefield cell wall polysaccharides that are expressed by these bacteria, the Group A Carbohydrate (GAC) for GAS and the Group B Carbohydrate (GBC) for GBS, are required for optimal hGIIA bactericidal efficacy by facilitating penetration through the peptidoglycan layer. Given the increased hGIIA resistance of antigen-modified or antigen-deficient streptococci, it will be of interest to determine potential regulatory mechanisms regarding expression of streptococcal Lancefield polysaccharides.

Introduction

Many important human bacterial pathogens are also common colonizers of mucosal barriers. Occasionally, such pathogens penetrate these physical barriers to invade the underlying tissues and cause infections. Antimicrobial molecules, sometimes also referred to as 'endogenous antibiotics of the host', are a critical part of the innate immune response to eradicate these intruders and clear the infection. In humans, one of the most potent bactericidal molecules against Gram-positive bacteria is the secreted enzyme human Group IIA phospholipase A2 (hGIIA) [1,2].

HGIIA belongs to a family of 11-12 secreted phospholipase A_2 ($sPLA_2$) enzymes, which are structurally related and hydrolyze various phospholipids [2–5]. In non-inflamed conditions, hGIIA serum levels are low and not sufficient to kill most Gram-positive bacteria [6]. However, sterile inflammation or infection increases hGIIA expression with concentrations reaching up to 1 µg/ml in serum [7], which is sufficient to kill most Gram-positive pathogens *in vitro*. A unique feature of hGIIA compared to other secreted Phospholipase A_2 family members is its high cationic charge, which is required for binding to negatively-charged surface structures and for penetration of the thick peptidoglycan layer surrounding Gram-positive bacteria [2,8,9]. The potent bactericidal activity of hGIIA against Gram-positive bacteria has been demonstrated both *in vitro*, using recombinant hGIIA, as well as *in vivo* using hGIIA transgenic mice [10–16]. To counter the bactericidal effects of hGIIA, pathogens have evolved different resistance mechanisms, for example by suppressing hGIIA expression [17,18] or by increasing the net positive charge of surface structures and membrane. The surface modifications include the addition of positively-charged D-alanine moieties to teichoic acid polymers by the highly conserved *dlt* operon to repulse hGIIA [8] and other cationic antimicrobials [19–22]. In addition, *Staphylococcus aureus* (*S. aureus*) modifies the charge of its bacterial membrane through the molecule MprF [23,24] by adding the cationic amino acid lysine to phosphatidylglycerol (PG), resulting in lysyl-PG [25]. In Group A *Streptococcus* (GAS), the enzyme sortase A (SrtA), a conserved

101 enzyme in Gram-positive bacteria that recognizes proteins with an LPXTG motif and
102 covalently attaches them to peptidoglycan [26,27], was shown to increase hGIIA resistance
103 [12].

104 Studies with recombinant hGIIA have highlighted differences in intrinsic hGIIA
105 susceptibility between different Gram-positive species, where *Bacillus subtilis* is killed in the
106 low ng/ml concentration range [28,29], and Group A *Streptococcus* (GAS) is one of the most
107 resistant species known to date [12]. Interestingly, this high resistance is not a common trait
108 of streptococcal pathogens since Group B *Streptococcus* (GBS) is killed by concentrations
109 that are approximately 500 times lower compared to those required to kill GAS [11,12].
110 Streptococci are historically classified by the expression of structurally different Lancefield
111 antigens [30]. Lancefield antigens are cell wall polysaccharides making up approximately
112 50% of the dry cell wall mass [31]. All GAS serotypes express the Lancefield Group A
113 carbohydrate (GAC), which consists of a polyrhamnose backbone with alternating *N*-
114 acetylglucosamine (GlcNAc) side chains [31], which are important for virulence [32]. In
115 contrast, all GBS serotypes express the Lancefield Group B carbohydrate (GBC), a multi-
116 antennary structure, containing rhamnose, galactose, GlcNAc, glucitol, and significant
117 amounts of phosphate [33]. Both streptococcal species are important human pathogens as
118 they can cause systemic infections associated with high mortality and morbidity [34–36].
119 Mouse infection models and *ex vivo* studies on human serum from infected patients
120 demonstrated the importance of hGIIA in defense against lethal infections with GAS and
121 GBS [11,12]. Given the importance of hGIIA in host defense against streptococci, we set out
122 to identify the molecular mechanisms that confer resistance to hGIIA using a comprehensive
123 and unbiased approach.

124

125

126 # Results

127 ## Globally-disseminated M1T1 GAS is highly resistant to hGIIA

128 A previous study found that GAS strains are among the most resistant Gram-positive
129 bacteria regarding hGIIA-mediated killing [12]. Mutation of *srtA* in the GAS strain JRS4, an
130 *emm6* serotype, increased hGIIA susceptibility by about 50-fold [12]. GAS M1T1 is a
131 globally-disseminated *emm1* clone that is most often responsible for invasive GAS infections
132 in industrialized countries [37,38] and was not included previously in hGIIA studies [12]. GAS
133 strain 5448, a representative M1T1 isolate, showed concentration-dependent killing by
134 recombinant human hGIIA, with an LD_{50} of 0.05 µg/ml (Fig 1A). Also, GAS M1T1 resistance
135 mechanisms against hGIIA at least partially overlap with GAS JRS4 *emm6*, since mutation
136 of *srtA* rendered GAS M1T1 approximately 35-fold more susceptible to hGIIA (Fig 1A) [12].

137 To study the activity of hGIIA in a more physiological setting, we spiked pooled
138 normal human serum with different concentrations of recombinant hGIIA. The addition of
139 serum potentiated hGIIA-mediated killing of GAS compared to the purified assay (Fig 1A) as
140 reflected by a 5-fold lower LD_{50} (0.01 ug/ml; Fig 1B). Interestingly, heat inactivation of serum
141 reduced the ability of hGIIA to kill GAS by 10-fold compared to active serum, indicating that
142 there are heat-labile factors in serum that potentiate hGIIA efficacy (Fig 1B). Endogenous
143 hGIIA present in normal human serum does not play a significant role since addition of the
144 hGIIA-specific inhibitor LY311727 [39] did not alter GAS growth in serum (Fig S1).

145 ## Identification of GAS genes that affect hGIIA susceptibility using Tn-seq

146 We set out to identify genes that affect hGIIA susceptibility of GAS M1T1 using the GAS
147 *Krmit* transposon mutant library [40]. To ensure complete coverage of the library in our
148 experiment, we optimized our hGIIA killing assay to support an inoculum of 10^7 CFU, using a
149 final concentration of 0.125 µg/ml hGIIA. The Tn-seq experiment with the GAS *Krmit*
150 transposon mutant library consisted of four non-exposed control samples and four hGIIA-
151 treated samples. Each sample contained on average approximately 30 million reads, of
152 which over 90% of the reads aligned once to the GAS M1T1 5448 reference genome (Table

153 S1) [41]. To quantify the number of transposon insertions per gene, we divided the reference
154 genome into 25 nucleotide windows, resulting in 73,182 windows, and mapped each read to
155 a specific window. More than 48% of the windows had at least one read aligned. We
156 identified one gene with an exceptionally high number of transposon insertions at a specific
157 part of the gene (M5005_Spy_1390), suggesting biased insertion of the transposon (Tables
158 S2, S3 and Fig S2). This gene was therefore excluded from further analysis. No other biased
159 transposon insertion sites were observed.

160 We identified 16 genes that contained a significantly different number of transposon
161 insertions after exposure to hGIIA as indicated by *P*-value of <0.05 (Benjamini-Hochberg
162 (BH) corrected; Fig 2A, Fig S3, and Tables S2-4). Nine of the 16 genes (56%) showed a
163 decrease in transposon insertions compared to untreated controls, indicating that the
164 products of the disrupted genes provide resistance against hGIIA-mediated GAS killing (Fig
165 2A, Fig S3, Table S3). Three susceptibility genes are located within the *dlt* operon
166 (M5005_Spy_1070, M5005_Spy_1072, M5005_Spy_1073), which is responsible for D-
167 alanylation of teichoic acids [42]. Consistently, this operon was previously linked to GAS
168 resistance against other cationic antimicrobials, such as LL-37 and hGIIA [8,43]. The other
169 six genes with significant fold decrease in transposon insertions are annotated as
170 hypothetical proteins (M5005_Spy_0918 and M5005_Spy_1794), a lactoylglutathione lyase
171 (M5005_Spy_0876), LytR (M5005_Spy_1474) of the LytR/CspA/Psr protein family, the
172 transcriptional regulator FabT (M5005_Spy_1495), and the NAD glycohydrolase inhibitor
173 (M5005_Spy_0140) (Fig S3 and Tables S2, S3).

174 Seven genes showed a relative increase in the number of transposon insertions after
175 hGIIA exposure, indicating that the products of these genes are important for hGIIA to exert
176 its bactericidal effect (Fig 2A, Fig. S3, Table S4). Five of the six genes (83%) mapped to two
177 gene clusters; one gene cluster is annotated as an ABC transporter (M5005_Spy_0939,
178 M5005_Spy_0940, M5005_Spy_0941) and the other gene cluster is the previously identified
179 12-gene cluster responsible for biosynthesis of the Group A carbohydrate (GAC) (Fig 2B)
180 [32]. Within the GAC gene cluster, *gacI* and *gacH* (M5005_Spy_0609 and

181 M5005_Spy_0610) showed significantly increased number of transposon insertions. The
182 small downstream gene *gacJ* (M5005_Spy_0611) also demonstrated a 3-fold increase,
183 however, the BH corrected *P*-value is slightly above 0.05. Other genes within the GAC gene
184 cluster are essential or crucial as described previously [40,44]. Finally, *guaB*
185 (M5005_Spy_1857) and the IIC component of a galactose-specific PTS system
186 (M5005_Spy_1399) were identified as their mutation may confer increased resistance to
187 hGIIA (Fig S3 and Tables S2, S4). Overall, the transposon library screen identified genes
188 that confer resistance or are important for the mechanisms of action of hGIIA.

189 HGIIA requires the GAC GlcNAc side chain to exert its bactericidal effect 190 against GAS

191 To validate the Tn-seq findings, we confirmed the involvement of three genes (*dltA*, *lytR*, and
192 *gacI*) by assessing hGIIA-mediated killing of previously generated GAS mutants [32,43,45].
193 Deletion of *dltA* and *lytR* indeed increased GAS susceptibility to hGIIA-mediated killing by
194 45-fold and 35-fold, respectively (Fig 3A and 3B). The *dltA* defect could be restored by re-
195 introduction of the gene on a plasmid (Fig 3A).

196 In contrast to *dltA* and *lytR*, mutation of *gacI*, which results in loss of the GAC
197 GlcNAc side chain [46], increased GAS resistance to hGIIA by approximately 10-fold
198 compared to the parental or *gacI*-complemented (*gacI**) strain (Fig 3C; LD_{50} = 0.5 μg/ml).
199 The GAC is conserved in all GAS serotypes. We therefore questioned whether deletion of
200 *gacI* would have a similar effect on the bactericidal efficacy of hGIIA in four other GAS
201 serotypes (M2, M3, M4, M28). In all serotypes, deletion of *gacI* increased resistance of GAS
202 to hGIIA by 5- to 50-fold (Fig 3D), indicating that hGIIA requires the GAC GlcNAc side chain
203 for optimal bactericidal efficacy in all genetic backgrounds tested.

204 Loss of the GAC GlcNAc side chain delays cell wall translocation of hGIIA

205 Our observation that GAS Δ*gacI* is more resistant to hGIIA implies that the GAC GlcNAc
206 moiety is important for the function of hGIIA. To assess whether loss of the GAC GlcNAc
207 side chain affected hGIIA binding to bacteria, we quantified binding of recombinant hGIIA to

208 GAS using a $sPLA_2$-specific antibody. At concentrations that are occasionally reached in
209 plasma during inflamed conditions (up to 1 μg/ml), binding of hGIIA was similar in the three
210 strains (Fig 4A). Only at concentrations of 5 μg/ml, hGIIA showed reduced interaction with
211 the *gacI* mutant compared to GAS WT and *gacI**-complemented strains (Fig 4A). The
212 contribution of differential hGIIA binding to GAS is therefore only relevant to specific
213 locations such as in tears which contain up to 30 μg/ml hGIIA [28]. Since hGIIA binding is
214 charge-dependent, we analyzed whether reduced binding at high hGIIA concentrations
215 could be caused by difference in surface charge. Using the highly cationic protein
216 cytochrome C, we indeed observed that the *gacI* mutant has a reduced negative surface
217 charge compared to GAS WT and the *gacI**-complemented strain (Fig 4B). In addition, we
218 analyzed whether hGIIA bound to the bacterial surface at a specific side using fluorescence
219 microscopy. hGIIA predominantly localized to the GAS cell poles (Fig 4C).

220 Cell wall architecture can significantly affect hGIIA cell wall penetration [2]. To assess
221 how absence of the GAC GlcNAc side chain affected hGIIA cell wall penetration, we
222 measured changes in membrane depolarization over time using the fluorescent voltage-
223 sensitive dye $DiOC_2(3)$ [47]. In this assay, membrane depolarization results in reduced red
224 fluorescence. HGIIA required at least 5 minutes to penetrate the GAS cell wall since no
225 changes in red fluorescence signal were observed at this time point for any of the strains
226 (Fig S4A). After 5 minutes, membrane depolarization occurred as visualized by diminished
227 red fluorescence (Fig 4D and Fig S4B, S4C) and was most pronounced at high hGIIA
228 concentrations for GAS WT and the *gacI**-complemented strain. Compared to these two
229 strains, the *gacI* mutant exhibits only slight membrane depolarization at all time points (Fig
230 4D and Fig S4). To determine how membrane depolarization correlates to membrane
231 permeabilization, we measured influx of the fluorescent DNA dye SYTOX green, which can
232 only enter damaged membranes [48]. As expected, hGIIA increased the SYTOX signal in
233 GAS WT and GAS *gacI** after approximately 15 minutes (Fig 4E and Fig S5). SYTOX
234 intensity continued to increase for 60 to 80 minutes and then plateaued. In sharp contrast,

235 SYTOX intensity in GAS Δ*gacI* increased at a much slower rate and never reached the
236 levels of GAS WT and GAS *gacI** after two hours. The fact that SYTOX influx in GAS Δ*gacI*
237 is significantly slower and reduced compared to GAS WT suggests that the GAC GlcNAc
238 side chain is essential for efficient trafficking of hGIIA through the GAS cell wall.

239 A recent study demonstrates that GacI is a membrane protein that is required for the
240 intracellular formation of undecaprenyl-P-GlcNAc [46]. Therefore, loss of GacI could alter
241 membrane composition and fluidity to impact the activity of hGIIA on the membrane. To
242 analyze whether phospholipid hydrolysis is affected in GASΔ*gacI*, we performed the SYTOX
243 influx assay on protoplasts [49]. Unlike the previous SYTOX results with intact bacteria,
244 protoplasts from WT, Δ*gacI* and *gacI** strains all became SYTOX positive (Fig 4F and Fig
245 S6), underlining our conclusion that the presence of the cell wall in the Δ*gacI* limits access of
246 hGIIA to the streptococcal membrane. Nonetheless, the significantly lower SYTOX in the
247 Δ*gacI* protoplasts compared to the WT and *gacI**-complemented protoplasts (Fig 4F and Fig
248 S6), suggest that the absence of GacI reduces degradation by hGIIA.

249 In summary, these results suggest that hGIIA requires an intact GAC to efficiently
250 migrate through the cell wall. In addition, the presence of GacI in the cell membrane
251 increases membrane degradation by hGIIA likely due to a difference in membrane fluidity.

252 GBC is important for hGIIA bactericidal activity against GBS

253 We wondered whether the importance of the GAC for hGIIA activity could be extended to
254 other streptococci such as GBS. As previously described, GBS are generally more sensitive
255 to hGIIA compared to GAS [12]. Indeed, killing of GBS strain NEM316 occurred at
256 substantially lower concentrations of hGIIA compared to GAS M1T1 (compare Fig 5A and
257 1A). We confirmed that killing depends on the catalytic activity of the enzyme since
258 introduction of an inactivating point mutation (H48Q; Fig 5B) or addition of the hGIIA-specific
259 inhibitor LY311727 abrogated all killing (Fig 5C). Just as the GAC is the molecular signature
260 for GAS, GBS uniquely express another Lancefield antigen, known as the Group B
261 Carbohydrate (GBC). The GBC is a more complicated structure compared to the GAC and

262 contains significant amounts of phosphate that introduce a negative charge. GBS lacking the
263 GBC, through deletion of *gbcO* [33], are at least 100-fold more resistant to hGIIA compared
264 to GBS WT (Fig 5A-C), and the phenotype is restored upon complementation with *gbcO* on
265 a plasmid (Fig 5A). We could reproduce the Δ*gbcO* phenotype by treating WT GBS with
266 tunicamycin, an inhibitor of *gbcO*-type transferases (Fig 5D) [33,50]. Finally, as observed in
267 GAS, fluorescence microscopy demonstrated that hGIIA bound to the poles of GBS WT (Fig
268 5E). In conclusion, these results highlight a key role for streptococcal Lancefield antigens in
269 the bactericidal effect of hGIIA.

270 Discussion

271 The resistance to acute phase protein hGIIA varies among Gram-positive bacteria, including
272 among closely-related streptococcal species. GAS, an important cause of lethal infection
273 worldwide, is among the most resistant bacteria, whereas GBS, an important cause of
274 neonatal sepsis and meningitis, is killed by hGIIA at concentrations that are approximately
275 500-fold lower [12]. For GAS, we confirmed the role of Sortase A and DltA and identified
276 LytR as hGIIA resistance factors. Importantly, the streptococcal Lancefield antigens, which
277 are characteristic cell wall polysaccharides, are structural requirements for the activity of
278 hGIIA in both GAS and GBS. Together, these results indicate that the precise cell wall
279 architecture is an important determinant for streptococcal hGIIA susceptibility.

280 HGIIA is approximately 10-fold more effective against GAS when spiked into normal
281 serum compared to heat-inactivated serum, and 5-fold more effective compared to our
282 'purified' system. This corresponds to a previous observation where hGIIA activity was
283 approximately 10-fold greater in serum or plasma than in the protein-depleted serum in
284 studies using *S. aureus* as the target pathogen [51]. This suggests the presence of a heat
285 labile protein in plasma that facilitates hGIIA-mediated killing of Gram-positive bacteria.
286 Heat-inactivation of serum is a well-established method to study the influence of the
287 complement system and also abolishes hGIIA activity in acute phase serum [52]. Since the
288 low basal levels of hGIIA in normal human serum are not sufficient to affect GAS viability,

289 the enhancement could indicate a synergistic effect between hGIIA and the complement
290 system. A recent study shows formation of the Membrane Attack Complex (MAC) on the
291 GAS surface without affecting bacterial viability [53]. It is therefore tempting to speculate that
292 MAC is deposited on Gram-positive bacteria so that bactericidal enzymes, such as hGIIA,
293 can reach the bacterial membrane more easily.

294 Sortase A, an enzyme that links LPXTG-containing proteins to peptidoglycan, is
295 known to be involved in GAS hGIIA resistance [12]. Whether a single or multiple LPXTG
296 proteins confer resistance is an unresolved question. Our study suggests that Sortase-A
297 mediated resistance is not caused by a single LPXTG protein since we did not identify a
298 single LPXTG-encoding gene in the Tn-seq screen (Table S5). Possibly, the underlying
299 mechanism is similar to the SrtA-dependent resistance of GAS to the antimicrobial peptide
300 cathelicidin [54], which depends on the accumulation of sorting intermediates at the bacterial
301 membrane. *SrtA* itself was not identified in the transposon library screen since the mutants
302 are lost in the competitive environment likely due to inherent defects in growth [40].

303 We identified and confirmed a role for the protein LytR in GAS hGIIA resistance. LytR
304 is a member of the LytR-CpsA-Psr (LCP) protein family, a conserved family of cell wall
305 assembly proteins in Gram-positive bacteria [55]. The GAS genome encodes two members
306 of this family, *lytR* (M5005_Spy_1474) and *psr* (M5005_Spy_1099). The fact that we only
307 identified LytR suggests that these proteins have non-redundant, but as yet unidentified,
308 functions. In several Gram-positive pathogens, including *Streptococcus pneumoniae*,
309 *Staphylococcus aureus* and *Bacillus anthracis*, LCP proteins anchor cell wall glycopolymers
310 such as wall teichoic acid (WTA), lipoteichoic acid (LTA) and capsular polysaccharides to
311 the cell envelope and are therefore critical for cell envelope assembly and virulence [55–60].
312 Additionally, *lytR* homologues in *Bacillus subtilis* and *Streptococcus mutans* contribute to cell
313 wall remodeling by increasing autolysin activity [61,62]. Previously, hGIIA activity has been
314 linked to autolysins; autolysin-deficient mutants are more resistant to hGIIA than their parent
315 strain [63]. A suggested mechanism is that hGIIA displaces positively-charged autolysins
316 from negatively-charged WTA and LTA, resulting in localized peptidoglycan digestion and

317 facilitated movement of hGIIA through the cell wall. Currently, the role of LytR either in GAS
318 cell wall assembly or in the regulation of autolysin activity is not known, but LytR-deficient
319 GAS display altered membrane integrity and potential [64], which could impact hGIIA
320 susceptibility. Moreover, *lytR* has been linked to GAS virulence in two different studies. In
321 the first study, *lytR* mutants in two different GAS M1 backgrounds showed a more virulent
322 phenotype in a subcutaneous murine model of infection, which was suggested to be a result
323 of increased SpeB activity [64]. LytR-mediated regulation of SpeB is unlikely to play a role in
324 hGIIA-mediated resistance in our experiments, since we used washed bacteria. In a more
325 recent study, *lytR* mutants in GAS 5448 M1T1 showed a competitive disadvantage for
326 fitness *in vivo* upon mixed subcutaneous infection [45]. Unfortunately, there is no information
327 regarding pathology or survival of the mice upon infection with the *lytR* mutant added alone
328 [45].

329 We also identified genes that render GAS more susceptible to hGIIA. *GacH*, *gacI*,
330 and *gacJ* are located in the biosynthesis gene cluster of the GAC, which may suggest that
331 the GAC is a target for hGIIA on the GAS surface. Mutation of *gacI* and *gacJ* results in loss
332 of the GAC GlcNAc side chain [32,46], whereas mutation of *gacH* does not affect side chain
333 formation [32]. We therefore hypothesize that the GAC provides hGIIA resistance through
334 two distinct mechanisms. First, a *gacI*/*J*-dependent mechanism that works through the GAS
335 GlcNAc side chain as important for binding and penetration of hGIIA to the cell membrane.
336 The second mechanism involves GacH but the underlying molecular aspects remain to be
337 determined. The first mechanism seems to conflict with our previous observations that
338 GlcNAc-deficient GAS have decreased virulence capacity due to increased neutrophil killing
339 and increased susceptibility to antimicrobials in serum including LL-37 [32]. However, hGIIA
340 would not have contributed to *in vitro* assays since we used non-inflamed serum or plasma
341 where basal hGIIA concentrations are too low to affect GAS viability [32]. The fact that *gacI*
342 mutants demonstrate reduced survival *in vivo* suggests that the benefits of expressing the
343 GlcNAc side chain outweigh the increased susceptibility to hGIIA. Since GAS already shows
344 high intrinsic resistance towards hGIIA there is no pressure to lose the GlcNAc side chain. It

345 might even be detrimental since it makes GAS more vulnerable to effects of other
346 antimicrobials or yet unidentified host defenses. In contrast to the GAC [31,65], the GBC is a
347 multi-antennary structure and contains anionic charge due to the presence of phosphate
348 [33]. For GBS, the increased hGIIA resistance in GBC-negative *gbcO* mutants is therefore
349 likely explained by the loss of negatively charged groups on the surface. This corresponds to
350 previous observations in *S. aureus*, where loss of the secondary cell wall glycopolymer
351 WTA, increased resistance to several antimicrobial proteins, including hGIIA [10].

352 Contrary to our expectations, fluorescence microscopy analysis showed that hGIIA
353 bound to the cell poles of both GAS and GBS. This binding pattern does not correspond to
354 the localization of the GAC and GBC, which are distributed over the entire cell wall as shown
355 by early electron microscopy studies [66,67]. Binding at the septa of dividing bacteria seems
356 a preferred binding site for bactericidal agents due to a high turnover of peptidoglycan which
357 would make penetration easier [68,69]. In addition, the septum is rich in anionic
358 phospholipids [70], a likely target for cationic hGIIA. Finally, the GAS ExPortal, a unique
359 microdomain in the GAS membrane that is enriched in anionic lipids, would be another
360 favored location of binding for the cationic hGIIA [71]. However, the ExPortal is distributed
361 asymmetrically across the GAS surface and not at the cell poles [71]. The fact that we
362 observe a similar binding pattern to GBS and GAS, may indicate that GAS and GBS express
363 a similar protein that localizes at the cell poles and is used by hGIIA as an initial docking
364 site. The exact reason for hGIIA binding at the cell poles remains to be determined.

365 Lack of the GAC GlcNAc side chain most profoundly affected penetration of hGIIA
366 through the cell wall, a mechanism that depends on charge [2,9]. Indeed, membrane
367 depolarization and permeabilization occurs at a much slower rate in the *gacI* mutant
368 compared to WT and complemented strains. This implies that the GAC GlcNAc side chain
369 facilitates penetration of hGIIA through the cell wall in what is referred to as an 'anionic
370 ladder process' [2]. Interestingly, the GAC does not contain any charged structures.
371 Therefore, the underlying mechanism may be linked to the previously mentioned autolysin
372 displacement from interaction with the GAC.

373 In conclusion, we show that the bactericidal agent hGIIA is able to kill GAS in a
374 complex serum environment. However, modification or removal of the Lancefield antigen
375 renders GAS more resistant to the bactericidal activity of hGIIA. Similarly, removing the
376 Lancefield antigen from GBS renders this species also more resistant to the bactericidal
377 activity of hGIIA. The Lancefield antigens, previously thought to be solely involved in
378 physiology, are thus critical cell wall structures for hGIIA to exert its bactericidal effect. The
379 Tn-seq data discussed in this paper provide exciting new insights into the resistance
380 mechanisms of GAS and encourage similar experiments in other streptococci species.
381 Disrupting the resistance mechanisms with therapeutic agents could possibly be sufficient to
382 provide our own immune system the upper hand in clearing invading streptococcal
383 pathogens.
384

385 ## Materials and Methods

386 ### Bacterial strains

387 The GAS M1T1 5448 strain was used in this study unless stated otherwise. The 5448Δ*gacI*
388 knockout and *gacI** complemented strain [32], the 5448Δ*lytR* [45] and the GAS serotypes
389 M2, M3, M4, and M28 and corresponding Δ*gacI* knockouts [72] were described previously.
390 Preparation and characterization of the GAS M1T1 5448 transposon library was described
391 previously by Le Breton et al., 2015 [40]. All GAS strains were grown in Todd-Hewitt broth
392 (Becton Dickinson) supplemented with 1% yeast extract (Oxoid; THY) as static cultures at
393 37 °C. Kanamycin (Sigma-Aldrich) was used at a concentration of 300 µg/ml when
394 appropriate. GBS NEM316 WT, Δ*gbcO* and the complemented strains Δ*gbcO*/pTCV were
395 kindly provided by Dr. Mistou [33].
396 Unless stated otherwise, overnight cultures of GAS were diluted and re-grown to
397 mid-log phase (OD_{600nm} = 0.4), washed and resuspended in HEPES solution (20 mM
398 HEPES, 2 mM Ca^{2+}, 1% BSA [pH 7.4]) solution at OD_{600nm} = 0.4 (~$1x10^8$ CFU/ml). For GBS
399 strains, overnight cultures of NEM316 WT, Δ*gbcO* and the complemented strains

400 Δ*gbcO*/pTCV were diluted in TH broth and grown to mid-log phase (OD_{620nm} = 0.4 for WT
401 and complemented strains, 0.25 for Δ*gbcO* mutant). Bacteria were then diluted in HEPES
402 solution and pushed rapidly through a 27-gauge needle, a process repeated three times, to
403 disrupt bacterial aggregates.

404 **Identification of GAS resistance determinants against hGIIA**

405 Recombinant hGIIA was produced as described previously [73]. The GAS M1T1 *Krmit*
406 transposon mutant library was grown to mid-log phase in 100 ml THY containing Km and
407 resuspended in HEPES solution to OD_{600nm}= 0.4. Four experimental replicates of 100 µl (~
408 $1x10^7$ CFU) were subsequently incubated in HEPES solution with or without 125 ng/ml
409 hGIIA for 1 hour at 37 °C. After incubation, 3 ml THY was added to all samples and
410 incubated at 37 °C until the mid-log phase was reached (recovery step). Cultures were
411 collected by centrifugation and used for isolation of genomic DNA (gDNA). gDNA was
412 isolated by phenol-chloroform extraction. Samples were barcoded and prepared for Tn-seq
413 sequencing as described previously [74]. Tn-seq sequencing was performed on Illumina
414 NextSeq500 (Sequencing facility University Medical Center, Utrecht, The Netherlands).

415 Tn-seq data analysis was performed as previously described [74]. In short, barcodes
416 were split using the Galaxy platform [75] and sequences were mapped to the GAS M1T1
417 5448 genome [41] using Bowtie 2 [76]. The genome was subsequently divided in 25-bp
418 windows and each alignment was sorted and indexed by IGV [77]. Insertions were counted
419 per window and then summed over the genes. Read counts per gene were adjusted to cover
420 only the first 90% of the gene since transposon insertions in the final 10% potentially do not
421 cause a knock-out phenotype. Then, read counts were normalized to the total number of
422 reads that mapped to the genome in each replicate, by calculating the normalized read-
423 count RKPM (Reads Per Kilobase per Million input reads; RKPM = (number of reads
424 mapped to a gene x 10^6) / (total mapped input reads in the sample x gene length in kbp)).
425 Cyber-T [78] was used to perform statistical analysis on the RKPM values. Genes that
426 contributed to either hGIIA susceptibility or hGIIA resistance were determined when the

427 Benjamini-Hochberg (BH) corrected *p*-value was <0.05.

428 **hGIIA susceptibility**

429 Mid-log streptococcal suspensions were diluted 1,000 times in HEPES solution and 10 µl
430 was added to sterile round-bottom 96 well plates (triplicates). Recombinant hGIIA or
431 catalytically-deficient hGIIA mutant enzyme H48Q was serially diluted in HEPES solution or
432 human serum and 10 µl aliquots were added to bacteria-containing wells. For hGIIA
433 inhibition experiments, 50 µM LY311727 was added to the HEPES solution or serum. For
434 GAS, samples were incubated for 2 hours at 37°C, without shaking, PBS was added and
435 samples were 10-fold serially diluted and plated on THY agar plates for quantification. For
436 GBS, bacteria were incubated with hGIIA at 37°C for 30 minutes, the samples were diluted
437 in PBS and plated onto blood agar plates. After overnight incubation 37°C, colony forming
438 units (CFU) were counted to calculate the survival rate (Survival (% of inoculum) = (counted
439 CFU * 100) / CFU count of original inoculum or Survival (%) = (counted CFU * 100) / CFU
440 count at 0 µg/ml hGIIA). For pharmacological inhibition of GBC expression, NEM316 WT
441 bacteria were grown to mid-log phase (OD_{620nm} = 0.4) in the presence of 0.5 mg/ml
442 tunicamycin (Sigma) and used in killing assays as described above.

443 **Membrane potential and permeability assays**

444 Changes in hGIIA-dependent membrane potential were determined using the membrane
445 potential probe $DiOC_2(3)$ (PromoKine) [47,79]. Bacterial suspensions (OD_{600nm}= 0.4) were
446 diluted 100 times (~$1x10^6$ CFU/ml), 100 µl aliquots were divided into eppendorf tubes and
447 incubated with serial dilutions of hGIIA. After incubation at 37°C, 3 mM $DiOC_2(3)$ was added
448 and incubated at room temperature for 5 minutes in the dark. Changes in green and red
449 fluorescence emissions were analyzed by flow cytometry.

450 Bacterial staining with the DNA stain SYTOX Green (Invitrogen) is a measurement
451 for membrane permeabilization and an indication of bacterial cell death [48]. Serial dilutions
452 of hGIIA in HEPES solutions were added to wells of a sterile flat-bottom 96 well plate.
453 Bacteria were resuspended in HEPES solution containing 1 µM SYTOX green (OD_{600nm} =

454 0.4) and added to hGIIA dilutions in a final volume of 100 µl. Fluorescence over time was
455 recorded using FLUOstar OPTIMA (green fluorescence 530 nm emission and excitation 488
456 nm) at 37°C.

457 **Surface charge determination**

458 Bacterial surface charge was determined as previously described [79]. Briefly, exponential
459 phase bacteria (OD_{600nm} = 0.4) were washed twice in 20 mM MOPS buffer [pH 7.0] and
460 adjusted to OD_{600nm} = 0.7. After a 10-fold concentration step, 200 µl bacterial aliquots were
461 added to 200 µg cytochrome c (from *Saccharomyces cerevisiae*, Sigma-Aldrich) in a sterile
462 96-well round-bottom plate. After 10 minutes at room temperature in the dark, the plate was
463 centrifuged, the supernatant was transferred to a sterile 96 well flat-bottom plate and
464 absorbance was recorded at 530 nm. The percentage of bound cytochrome c was
465 calculated using samples containing MOPS buffer only (100% binding) and samples
466 containing MOPS buffer and cytochrome c (0% binding).

467 **hGIIA surface binding**

468 To determine hGIIA surface binding, 12.5 µl of bacterial cultures in mid-log phase (OD_{600nm} =
469 0.4) were added to wells of a sterile 96-well round-bottom plate (triplicates). hGIIA was
470 serially diluted in HEPES solution without Ca^{2+} and added to the bacteria at indicated
471 concentrations. After 30 minutes incubation at 4°C, bacteria were collected by centrifugation
472 and resuspended in HEPES solution without Ca^{2+} containing 1:300 dilution of anti-$sPLA_2$
473 antibody (Merck Millipore) [28]. After incubation at 4°C for 30 minutes, the samples were
474 washed and incubated with a 1:1,000 dilution of FITC-labeled goat-anti-mouse IgG
475 (SouthernBiotech). After washing with HEPES solution without Ca^{2+}, samples were fixed
476 with 1% paraformaldehyde and fluorescence was recorded by flow cytometry (FACSVerse,
477 BD Biosciences).

478 **Fluorescence microscopy**

479 To analyze hGIIA surface localization by microscopy, bacteria were grown in 10 ml broth to
480 mid-log phase and washed with 0.1 M $NaHCO_3$ [pH 9]. For GBS, the bacterial septa were
481 stained by addition of a 1:1 mixture of Vancomycin bodipy® FL conjugate (Invitrogen,
482 V34550) and vancomycin (Sigma) at a final concentration of 1.25 µg/ml, during the last
483 generation time of growth. The surface of GBS was stained with Alexa Fluor® 350
484 Carboxylic acid Succinimidyl ester (Molecular Probes by Life Technologies, A10168) for 1
485 hour in room temperature. Bacteria were then resuspended in 500 µl HEPES solution and
486 the suspension was divided over two tubes. A final concentration of 10 µg/ml hGIIA H48Q
487 was added to one tube and HEPES solution to the other before a 30 minute incubation at
488 room temperature. The samples were washed and resuspended in 200 µl HEPES solution,
489 then again divided to two tubes. A mouse anti-human hGIIA monoclonal antibody (Clone
490 SCACC353 Cayman Chemical) or an IgG1 isotype control (mouse anti human IgA clone
491 6E2C1, DAKO) was added to a final concentration of 10 µg/ml to the bacterial suspensions
492 and incubated at RT. After washing, the samples were incubated with 8 µg/ml of Alexa
493 Flour® 594 goat anti-mouse IgG1 (Molecular Probes by Life Technologies, A21125). After
494 30 min incubation, the samples were washed in HEPES solution and fixed in 4%
495 paraformaldehyde. Ten µl of bacterial suspension were mounted onto microscopic slides
496 (VWR) using MOWIOL (Sigma) mounting medium before viewing the samples using Zeiss
497 Axiovert 200M microscope. Pictures were captured using a 63× objective and the
498 AXIOVISION 4.8 software.
499

500 **Hydrolysis of membrane phospholipids**

501 To determine hGIIA efficacy in hydrolyzing membrane phospholipids, the membrane
502 permeabilization assay was modified for protoplasts. Mid-log bacterial suspension were
503 prepared in in protoplast buffer (20% sucrose, 20 mM Tris-HCl, 10 mM $MgCl_2$, 2 mM $CaCl_2$
504 [pH 7.4]) containing 1.4 units/µl mutanolysin (Sigma-Aldrich) [49,80,81]. After incubation for
505 1 hour at 37°C, protoplasts were collected by centrifugation (1,200 rpm 15 minutes) and

506 resuspended in protoplast buffer to an OD_{600nm} = 0.4. Pore formation by hGIIA was
507 monitored using SYTOX Green as described above.
508

509 **Statistical analysis**

510 GraphPad Prism 6 was used to perform statistical analysis. An unpaired two-tailed Student's
511 *t*-test was used to compare the means of two groups. A 2-way ANOVA with Bonferroni
512 multiple comparison test was used to compare multiple groups. Data shown are mean ± SD.
513

514 **References**

515 1. Nevalainen TJ, Graham GG, Scott KF. Antibacterial actions of secreted
516 phospholipases A2. Review. Biochim Biophys Acta - Mol Cell Biol Lipids. 2008;1781:
517 1–9. doi:10.1016/j.bbalip.2007.12.001

518 2. Weiss JP. Molecular determinants of bacterial sensitivity and resistance to
519 mammalian Group IIA phospholipase A2. Biochim Biophys Acta - Biomembr. Elsevier
520 B.V.; 2015;1848: 3072–3077. doi:10.1016/j.bbamem.2015.05.018

521 3. Gelb MH, Jain MK, Hanel AM, Berg OG. Interfacial enzymology of glycerolipid
522 hydrolases: lessons from secreted phospholipases A2. Annu Rev Biochem. 1995;64:
523 653–88. doi:10.1146/annurev.bi.64.070195.003253

524 4. Lambeau G, Gelb MH. Biochemistry and Physiology of Mammalian Secreted
525 Phospholipases A_2. Annu Rev Biochem. 2008;77: 495–520.
526 doi:10.1146/annurev.biochem.76.062405.154007

527 5. Murakami M, Lambeau G. Emerging roles of secreted phospholipase A2 enzymes: An
528 update. Biochimie. Elsevier Masson SAS; 2013;95: 43–50.
529 doi:10.1016/j.biochi.2012.09.007

530 6. Nevalainen T, Kortesuo P. Immunochemical detection of group I and group II
531 phospholipases A2 in human serum. Clin Chem. 1992;38: 1824–1829. Available:
532 http://www.clinchem.org/content/38/9/1824.short

533 7. Green J, Smith G, Buchta R, Lee R, Ho K, Rajkovic I, et al. Circulating phospholipase
534 A2 activity associated with sepsis and septic shock is indistinguishable from that
535 associated with rheumatoid arthritis. Inflammation. 1991;15: 355–367.

536 8. Koprivnjak T, Peschel A, Gelb MH, Liang NS, Weiss JP. Role of charge properties of
537 bacterial envelope in bactericidal action of human Group IIA phospholipase A2
538 against *Staphylococcus aureus*. J Biol Chem. 2002;277: 47636–47644.
539 doi:10.1074/jbc.M205104200

540 9. Beers SA, Buckland AG, Koduri RS, Cho W, Gelb MH, Wilton DC. The antibacterial
541 properties of secreted phospholipases A2: A major physiological role for the group IIA
542 enzyme that depends on the very high pI of the enzyme to allow penetration of the
543 bacterial cell wall. J Biol Chem. 2002;277: 1788–1793. doi:10.1074/jbc.M109777200

544 10. Koprivnjak T, Weidenmaier C, Peschel A, Weiss JP. Wall teichoic acid deficiency in

545 *Staphylococcus aureus* confers selective resistance to mammalian group IIA
546 phospholipase A2 and human β-defensin 3. Infect Immun. 2008;76: 2169–2176.
547 doi:10.1128/IAI.01705-07

548 11. Movert E, Wu Y, Lambeau G, Kahn F, Touqui L, Areschoug T. Secreted group IIA
549 phospholipase A2 protects humans against the Group B *Streptococcus*: Experimental
550 and clinical evidence. J Infect Dis. 2013;208: 2025–2035. doi:10.1093/infdis/jit359

551 12. Movert E, Wu Y, Lambeau G, Touqui L, Areschoug T. A novel bacterial resistance
552 mechanism against human group IIA-secreted phospholipase A2: role of
553 *Streptococcus pyogenes* sortase A. J Immunol. 2011;187: 6437–46.
554 doi:10.4049/jimmunol.1100499

555 13. Gelb MH, Valentin E, Ghomashchi F, Lazdunski M, Lambeau G. Cloning and
556 recombinant expression of a structurally novel human secreted phospholipase A2. J
557 Biol Chem. 2000;275: 39823–39826. doi:10.1074/jbc.C000671200

558 14. Koduri RS, Gronroos JO, Laine VJ, Le Calvez C, Lambeau G, Nevalainen TJ, et al.
559 Bactericidal properties of human and murine groups I, II, V, X, and XII secreted
560 phospholipases A(2). J Biol Chem. 2002;277: 5849–5857.
561 doi:10.1074/jbc.M109699200

562 15. Piris-Gimenez A, Paya M, Lambeau G, Chignard M, Mock M, Touqui L, et al. In vivo
563 protective role of human group IIa phospholipase A2 against experimental anthrax. J
564 Immunol. 2005;175: 6786–6791. doi:10.4049/jimmunol.175.10.6786

565 16. Pernet E, Guillemot L, Burgel PR, Martin C, Lambeau G, Sermet-Gaudelus I, et al.
566 *Pseudomonas aeruginosa* eradicates *Staphylococcus aureus* by manipulating the
567 host immunity. Nat Commun. 2014;5. doi:10.1038/ncomms6105

568 17. Raymond B, Leduc D, Ravaux L, Le Goffic R, Candela T, Raymondjean M, et al.
569 Edema toxin impairs anthracidal phospholipase A2 expression by alveolar
570 macrophages. PLoS Pathog. 2007;3: 1907–1917. doi:10.1371/journal.ppat.0030187

571 18. Raymond B, Ravaux L, Mémet S, Wu YZ, Sturny-Leclère A, Leduc D, et al. Anthrax
572 lethal toxin down-regulates type-IIA secreted phospholipase A2expression through
573 MAPK/NF-κB inactivation. Biochem Pharmacol. 2010;79: 1149–1155.
574 doi:10.1016/j.bcp.2009.11.023

575 19. Weidenmaier C, Peschel A, Kempf VAJ, Lucindo N, Yeaman MR, Bayer AS.
576 DltABCD- and MprF-mediated cell envelope modifications of *Staphylococcus aureus*
577 confer resistance to platelet microbicidal proteins and contribute to virulence in a
578 rabbit endocarditis model. Microbiology. 2005;73: 8033–8038.
579 doi:10.1128/IAI.73.12.8033

580 20. McBride SM, Sonenshein AL. The dlt operon confers resistance to cationic
581 antimicrobial peptides in *Clostridium difficile*. Microbiology. 2011;157: 1457–1465.
582 doi:10.1099/mic.0.045997-0

583 21. Abachin E, Poyart C, Pellegrini E, Milohanic E, Fiedler F, Berche P, et al. Formation
584 of D-alanyl-lipoteichoic acid is required for adhesion and virulence of *Listeria*
585 *monocytogenes*. Mol Microbiol. 2002;43: 1–14. doi:10.1046/j.1365-
586 2958.2002.02723.x

587 22. Fisher N, Shetron-Rama L, Herring-Palmer A, Heffernan B, Bergman N, Hanna P.
588 The dltABCD operon of *Bacillus anthracis* Sterne is required for virulence and
589 resistance to peptide, enzymatic, and cellular mediators of innate immunity. J
590 Bacteriol. 2006;188: 1301–1309. doi:10.1128/JB.188.4.1301-1309.2006

591 23. Ernst CM, Peschel A. Broad-spectrum antimicrobial peptide resistance by MprF-
592 mediated aminoacylation and flipping of phospholipids. Mol Microbiol. 2011;80: 290–
593 299. doi:10.1111/j.1365-2958.2011.07576.x

24. Nevalainen TJ, Haapamäki MM, Grönroos JM. Roles of secretory phospholipases A2 in inflammatory diseases and trauma. Biochim Biophys Acta. 2000;1488: 83–90. doi:10.1016/S1388-1981(00)00112-8

25. Ernst CM, Kuhn S, Slavetinsky CJ, Krismer B, Heilbronner S, Gekeler C, et al. The lipid-modifying multiple peptide resistance factor is an oligomer consisting of distinct interacting synthase and flippase subunits. MBio. 2015;6: 1–9. doi:10.1128/mBio.02340-14

26. Mazmanian SK. *Staphylococcus aureus* Sortase, an enzyme that anchors surface proteins to the cell wall. Science 1999;285: 760–763. doi:10.1126/science.285.5428.760

27. Hendrickx APA, Budzik JM, Oh S-Y, Schneewind O. Architects at the bacterial surface - sortases and the assembly of pili with isopeptide bonds. Nat Rev Microbiol. Nature Publishing Group; 2011;9: 166–176. doi:10.1038/nrmicro2520

28. Qu X, Lehrer RI. Secretory Phospholipase A2 is the principal bactericide for staphylococci and other Gram-positive bacteria in human tears. Infect Immun. 1998;66: 2791–2797.

29. Weinrauch Y, Elsbach P, Madsen LM, Foreman A, Weiss J. The potent anti-*Staphylococcus aureus* activity of a sterile rabbit inflammatory fluid is due to a 14-kD phospholipase A2. J Clin Invest. 1996;97: 250–257. doi:10.1172/JCI118399

30. Lancefield RC. A Serological differentiation of human and other groups of hemolytic streptococci. J Exp Med. 1933;57: 571–595.

31. McCarthy M. The lysis of Group A hemolytic streptococci by extracellular enzymes of *Streptomyces albus*. II. Nature of the cellular substrate attacked by the lytic Enzymes. J Exp Med. 1952;96: 569–580.

32. Van Sorge NM, Cole JN, Kuipers K, Henningham A, Aziz RK, Kasirer-Friede A, et al. The classical lancefield antigen of group A *Streptococcus* is a virulence determinant with implications for vaccine design. Cell Host Microbe. 2014;15: 729–740. doi:10.1016/j.chom.2014.05.009

33. Caliot É, Dramsi S, Chapot-Chartier M-P, Courtin P, Kulakauskas S, Péchoux C, et al. Role of the Group B antigen of *Streptococcus agalactiae*: a peptidoglycan-anchored polysaccharide involved in cell wall biogenesis. PLoS Pathog. 2012; 8: e1002756. doi:10.1371/journal.ppat.1002756

34. Carapetis JR, Steer AC, Mulholland EK, Weber M. The global burden of group A streptococcal diseases. Lancet Infect Dis. 2005;5: 685–694. doi:10.1016/S1473-3099(05)70267-X

35. High KP, Edwards MS, Baker CJ. Group B Streptococcal infections in elderly adults. Clin Infect Dis. 2005;41: 839–847. doi:10.1086/432804

36. Edmond KM, Kortsalioudaki C, Scott S, Schrag SJ, Zaidi AK, Cousens S, et al. Group B streptococcal disease in infants aged younger than 3 months: Systematic review and meta-analysis. Lancet. 2012;379: 547–556. doi:10.1016/S0140-6736(11)61651-6

37. Kaul R, McGeer A, Low DE, Green K, Schwartz B, Simor AE, et al. Population-based surveillance for group A streptococcal necrotiziug fasciitis: Clinical features, prognostic indicators, and microbiologic analysis of seventy-seven cases. Am J Med. 1997;103: 18–24. doi:10.1016/S0002-9343(97)00160-5

38. Davies HD, McGeer A, Schwartz B, Green K, Cann D, Simor AE, et al. Invasive Group A Streptococcal infections in Ontario , Canada. N Engl J Med. 1996;335: 547–554.

39. Attalah HL, Wu Y, Alaoui-El-Azher M, Thouron F, Koumanov K, Wolf C, et al. Induction of type-IIA secretory phospholipase A2 in animal models of acute lung

643 injury. Eur Respir J. 2003;21: 1040–1045. doi:10.1183/09031936.03.00093002

644 40. Le Breton Y, Belew AT, Valdes KM, Islam E, Curry P, Tettelin H, et al. Essential
645 genes in the core genome of the human pathogen *Streptococcus pyogenes*. Sci Rep.
646 2015;5: 9838. doi:10.1038/srep09838

647 41. Fiebig A, Loof TG, Babbar A, Itzek A, Koehorst JJ, Schaap PJ, et al. Comparative
648 Genomics of *Streptococcus pyogenes* M1 isolates differing in virulence and
649 propensity to cause systemic infection in mice. Int J Med Microbiol. 2015;305: 532–
650 543. doi:10.1016/j.ijmm.2015.06.002

651 42. Peschel A, Otto M, Jack RW, Kalbacher H, Jung G, Götz F. Inactivation of the dlt
652 operon in *Staphylococcus aureus* confers sensitivity to defensins, protegrins, and
653 other antimicrobial peptides. J Biol Chem. 1999;274: 8405–8410.
654 doi:10.1074/JBC.274.13.8405

655 43. Kristian SA, Datta V, Weidenmaier C, Kansal R, Fedtke I, Peschel A, et al. D-
656 Alanylation of teichoic acids promotes Group A *Streptococcus* antimicrobial peptide
657 resistance, neutrophil survival, and epithelial cell invasion. J Bacteriol. 2005;187:
658 6719–6725. doi:10.1128/JB.187.19.6719

659 44. Le Breton Y, Mistry P, Valdes KM, Quigley J, Kumar N, Tettelin H, et al. Genome-
660 wide identification of genes required for fitness of Group A *Streptococcus* in human
661 blood. Infect Immun. 2013;81: 862–875. doi:10.1128/IAI.00837-12

662 45. Le Breton Y, Belew AT, Freiberg JA, Sundar GS, Islam E, Lieberman J, et al.
663 Genome-wide discovery of novel M1T1 Group A streptococcal determinants important
664 for fitness and virulence during soft-tissue infection. PLoS Pathog. 2017;13: 1–28.
665 doi:10.1371/journal.ppat.1006584

666 46. Rush JS, Edgar RJ, Deng P, Chen J, Zhu H, van Sorge NM, et al. The molecular
667 mechanism of N-acetylglucosamine side-chain attachment to the Lancefield Group A
668 carbohydrate in *Streptococcus pyogenes*. J Biol Chem. 2017;292: jbc.M117.815910.
669 doi:10.1074/jbc.M117.815910

670 47. Shapiro HM. Membrane potential estimation by flow cytometry. Methods. 2000;21:
671 271–279. doi:10.1006/meth.2000.1007

672 48. Saar-Dover R, Bitler A, Nezer R, Shmuel-Galia L, Firon A, Shimoni E, et al. D-
673 Alanylation of lipoteichoic acids confers resistance to cationic peptides in Group B
674 *Streptococcus* by increasing the cell wall density. PLoS Pathog. 2012;8.
675 doi:10.1371/journal.ppat.1002891

676 49. Albertí S, Ashbaugh CD, Wessels MR. Structure of the *has* operon promoter and
677 regulation of hyaluronic acid capsule expression in Group A *Streptococcus*. Mol
678 Microbiol. 1998;28: 343–353. doi:10.1046/j.1365-2958.1998.00800.x

679 50. Campbell J, Singh AK, Santa Maria JP, Kim Y, Brown S, Swoboda JG, et al. Synthetic
680 lethal compound combinations reveal a fundamental connection between wall teichoic
681 acid and peptidoglycan biosyntheses in *Staphylococcus aureus*. ACS Chem Biol.
682 2011;6: 106–116. doi:10.1021/cb100269f

683 51. Weinrauch Y, Abad C, Liang NS, Lowry SF, Weiss J. Mobilization of potent plasma
684 bactericidal activity during systemic bacterial challenge: role of Group IIA
685 Phospholipase A2. J Clin Invest. 1998;102: 633–638. doi:10.1172/JCI3121

686 52. Grönroos JO, Salonen JH, Viander M, Nevalainen TJ, Laine VJO. Roles of group IIA
687 phospholipase A2 and complement in killing of bacteria by acute phase serum. Scand
688 J Immunol. 2005;62: 413–419. doi:10.1111/j.1365-3083.2005.01678.x

689 53. Berends ETM, Dekkers JF, Nijland R, Kuipers A, Soppe JA, van Strijp JAG, et al.
690 Distinct localization of the complement C5b-9 complex on Gram-positive bacteria. Cell
691 Microbiol. 2013;15: 1955–1968. doi:10.1111/cmi.12170

692 54. Raz A, Tanasescu AM, Zhao AM, Serrano A, Alston T, Sol A, et al. *Streptococcus*
693 *pyogenes* sortase mutants are highly susceptible to killing by host factors due to
694 aberrant envelope physiology. PLoS One. 2015;10: 1–30.
695 doi:10.1371/journal.pone.0140784

696 55. Kawai Y, Marles-Wright J, Cleverley RM, Emmins R, Ishikawa S, Kuwano M, et al. A
697 widespread family of bacterial cell wall assembly proteins. EMBO J. 2011;30: 4931–
698 4941. doi:10.1038/emboj.2011.358

699 56. Dengler V, Meier PS, Heusser R, Kupferschmied P, Fazekas J, Friebe S, et al.
700 Deletion of hypothetical wall teichoic acid ligases in *Staphylococcus aureus* activates
701 the cell wall stress response. FEMS Microbiol Lett. 2012;333: 109–120.
702 doi:10.1111/j.1574-6968.2012.02603.x

703 57. Chan YGY, Frankel MB, Dengler V, Schneewind O, Missiakasa D. *Staphylococcus*
704 *aureus* mutants lacking the lytr-cpsa-Psr family of enzymes release cell wall teichoic
705 acids into the extracellular medium. J Bacteriol. 2013;195: 4650–4659.
706 doi:10.1128/JB.00544-13

707 58. Chan YGY, Kim HK, Schneewind O, Missiakas D. The capsular polysaccharide of
708 *Staphylococcus aureus* is attached to peptidoglycan by the LytR-CpsA-Psr (LCP)
709 family of enzymes. J Biol Chem. 2014;289: 15680–15690.
710 doi:10.1074/jbc.M114.567669

711 59. Zilla ML, Chan YGY, Lunderberg JM, Schneewind O, Missiakas D. LytR-CpsA-Psr
712 enzymes as determinants of *Bacillus anthracis* secondary cell wall polysaccharide
713 assembly. J Bacteriol. 2015;197: 343–353. doi:10.1128/JB.02364-14

714 60. Harrison J, Lloyd G, Joe M, Lowary TL, Reynolds E, Walters-Morgan H, et al. Lcp1 is
715 a phosphotransferase responsible for ligating arabinogalactan to peptidoglycan in
716 *Mycobacterium tuberculosis*. MBio. 2016;7: 1–12. doi:10.1128/mBio.00972-16

717 61. Lazarevic V, Margot P, Soldo B, Karamata D. Sequencing and analysis of the *Bacillus*
718 *subtilis* lytRABC divergon: a regulatory unit encompassing the structural genes of the
719 N-acetylmuramoyl-L-alanine amidase and its modifier. J Gen Microbiol. 1992;138:
720 1949–1961. doi:10.1099/00221287-138-9-1949

721 62. Chatfield CH, Koo H, Quivey RG. The putative autolysin regulator LytR in
722 *Streptococcus mutans* plays a role in cell division and is growth-phase regulated.
723 Microbiology. 2005;151: 625–631. doi:10.1099/mic.0.27604-0

724 63. Foreman-Wykert AK, Weinrauch Y, Elsbach P, Weiss J. Cell-wall determinants of the
725 bactericidal action of group IIA phospholipase A2 against Gram-positive bacteria. J
726 Clin Invest. 1999;103: 715–21. doi:10.1172/JCI5468

727 64. Minami M, Ichikawa M, Ohta M, Hasegawa T. The cell envelope-associated protein,
728 LytR, regulates the cysteine protease SpeB in *Streptococcus pyogenes*. Apmis.
729 2012;120: 417–426. doi:10.1111/j.1600-0463.2011.02847.x

730 65. McCarty M. Variation in the group-specific carbohydrate of Group A Streptococci. II.
731 studies on the chemical basis for serological specificity of the carbohydrates. J Exp
732 Med. 1956;104: 629–643.

733 66. Swanson J, Gotschlich EC. Electron microscopy studies on Streptococci II. Group A
734 Carbohydrate. J Exp Med. 1973;138: 245–258.

735 67. Wagner M, Wagner B, Kubín VR. Immunoelectron microscopic study of the location of
736 group-specific and type-specific polysaccharide antigens on isolated walls of group B
737 streptococci. J Gen Microbiol. 1980;120: 369–76. Available:
738 http://www.ncbi.nlm.nih.gov/pubmed/7014772

739 68. Sochacki KA, Barns KJ, Bucki R, Weisshaar JC. Real-time attack on single
740 *Escherichia coli* cells by the human antimicrobial peptide LL-37. Proc Natl Acad Sci.

741 2011;108: E77–E81. doi:10.1073/pnas.1101130108

742 69. Rangarajan N, Bakshi S, Weisshaar JC. Localized permeabilization of *E. coli*
743 membranes by the antimicrobial peptide Cecropin A. Biochemistry. 2013;52: 6584–
744 6594. doi:10.1021/bi400785j

745 70. Mileykovskaya E, Dowhan W. Cardiolipin membrane domains in prokaryotes and
746 eukaryotes. Biochim Biophys Acta - Biomembr. 2009;1788: 2084–2091.
747 doi:10.1016/j.bbamem.2009.04.003

748 71. Rosch JW, Hsu FF, Caparon MG. Anionic lipids enriched at the ExPortal of
749 *Streptococcus pyogenes*. J Bacteriol. 2007;189: 801–6. doi:10.1128/JB.01549-06

750 72. Henningham A, Davies MR, Uchiyama S, Van Sorge NM, Lund S, Chen KT, et al.
751 Virulence role of the GlcNAc side chain of the Lancefield cell wall carbohydrate
752 antigen in non-M1-serotype Group A *Streptococcus*. MBio. 2018;9: 1–12.

753 73. Ghomashchi F, Brglez V, Payré C, Jeammet L, Bezzine S, Gelb MH, et al.
754 Preparation of the full set of recombinant mouse- and human-secreted
755 phospholipases A2. 1st ed. Methods in Enzymology. Elsevier Inc.; 2017.
756 doi:10.1016/bs.mie.2016.10.034

757 74. Zhang X, de Maat V, Guzman Prieto AM, Prajsnar TK, Bayjanov JR, de Been M, et al.
758 Fitness determinants of vancomycin-resistant *Enterococcus faecium* during growth in
759 human serum. MBC genomics. BMC Genomics; 2017;18: 1–12. doi:10.1101/101329

760 75. Goecks J, Nekrutenko A, Taylor J, Galaxy Team T. Galaxy: a comprehensive
761 approach for supporting accessible, reproducible, and transparent computational
762 research in the life sciences. Genome Biol. 2010;11: R86. doi:10.1186/gb-2010-11-8-
763 r86

764 76. Langmead B, Salzberg SL. Fast gapped-read alignment with Bowtie 2. Nat Methods.
765 2012;9: 357–359. doi:10.1038/nmeth.1923

766 77. Robinson JT, Thorvaldsdóttir H, Winckler W, Guttman M, Lander ES, Gets G, et al.
767 Integrative Genomics Viewer. Nat Biotechnol. 2013;29: 24–26. doi:10.1038/nbt0111-
768 24

769 78. Baldi P, Long AD. A Bayesian framework for the analysis of microarray expression
770 data: regularized t-test and statistical inferences of gene changes. Bioinformatics.
771 2001;17: 509–519. doi:10.1093/bioinformatics/17.6.509

772 79. Carvalho F, Atilano ML, Pombinho R, Covas G. L-Rhamnosylation of *Listeria*
773 *monocytogenes* wall teichoic acids promotes resistance to antimicrobial peptides by
774 delaying Interaction with the membrane. 2015; 1–29.
775 doi:10.1371/journal.ppat.1004919

776 80. Yokogawa K, Kawata S, Takemura T, Yoshimura Y. Purification and properties of lytic
777 Enzymes from *Streptomyces globisporus* 1829. Agr Biol Chem. 1975;39: 1533–1543.

778 81. Calandra GB, Cole RM. Lysis and protoplast formation of group B streptococci by
779 mutanolysin. Infect Immun. 1980;28: 1033–1037.

780

781 # Figure legends

782 **Fig 1. GAS M1T1 is killed by recombinant hGIIA, which is enhanced in human serum.**

783 (A) GAS M1T1 5448 is killed by hGIIA in a dose-dependent manner. Mutation of *srtA*

784 renders 5448 more susceptible to hGIIA killing. (B) A heat-labile factor in serum enhances

785 the ability of hGIIA to kill GAS. Data represent mean +/- SD of three independent
786 experiments. *, $p > 0.05$; ***, $p > 0.001$.

787 **Fig 2. Identifying GAS mutants with different hGIIA susceptibility by Tn-seq analysis.**
788 (A) Average log-fold change of transposon insertions in genes of the hGIIA-treated group
789 versus the control group. Grey dots represent genes without significant fold change after
790 hGIIA treatment. Green and orange dots represent genes with significantly increased and
791 reduced transposon insertions after hGIIA exposure, respectively. Significant hits have a
792 calculated BH corrected $p < 0.05$. (B) Circos representation of the average transposon
793 insertions of genes within the GAC gene cluster. All genes within this cluster, except for
794 *gacI*, *gacJ*, and *gacH*, were previously identified as essential [40]. For *gacI* and *gacH*, the
795 fold change shown is significant (BH corrected $p < 0.05$), whereas for *gacJ* the fold change
796 is not significant (BH corrected $p = 0.16$).

797 **Fig 3. Mutation of *dltA* and *lytR* renders GAS more susceptible to hGIIA, whereas**
798 **mutation of *gacI* increases hGIIA resistance in multiple GAS serotypes.** Deletion of (A)
799 *dltA* or (B) *lytR* increases GAS susceptibility to hGIIA-mediated killing in a concentration-
800 dependent manner. Deletion of *gacI* renders GAS more resistant to hGIIA-mediated killing
801 as shown for (C) 5448 and (D) other tested GAS serotypes. Data represent mean +/- SD of
802 three independent experiments. *, $p > 0.05$; **, $p > 0.01$; ***, $p > 0.001$.

803 **Fig 4. Lack of the GAC GlcNAc side chain delays hGIIA cell wall translocation.** (A)
804 Detection of hGIIA binding to GAS 5448 by flow cytometry. (B) Deletion of *gacI* affects
805 surface charge of GAS as determined in cationic cytochrome c binding assay. (C)
806 Localization of hGIIA (H48Q) on GAS 5448 was analyzed by fluorescence microscopy (+)
807 and quantified based on analysis of 10 fields including 307 stained cells from two separate
808 experiments. As control, H48Q hGIIA was omitted (-). hGIIA was detected with a mouse
809 anti-human hGIIA monoclonal antibody or an IgG1 isotype as negative control.
810 Representative cells are shown. (D) Effect of hGIIA on GAS membrane potential after 2 hour

811 incubation. Decreased PerCP signal indicates a disrupted membrane potential. (E) SYTOX
812 green uptake over time by GAS strains or (F) GAS protoplasts after incubation with
813 recombinant hGIIA. Data represent mean +/- SD of three independent experiments. ns = not
814 significant, *, $p > 0.05$; **, $p > 0.01$; ***, $p > 0.001$.

815 **Fig 5. GBS lacking the GBC are resistant to hGIIA.** (A) HGIIA kills GBS strain NEM316
816 WT but not Δ*gbcO* in a concentration-dependent manner and phenotype is restored in
817 complemented strain ΔgbcO/pTCV. The killing is represented as the percentage of CFU
818 surviving after hGIIA exposure compared to the inoculum. GBS killing is prevented when (B)
819 exposed to catalytically inactive hGIIA H48Q and (C) by the hGIIA-specific inhibitor
820 LY311727. (D) Treatment of NEM316 WT with the *gbcO*-type inhibitor tunicamycin
821 reproduces the Δ*gbcO* phenotype with regard to hGIIA-mediated killing GBS more resistant
822 to hGIIA-mediated killing. (E) Visualization of bacteria-bound hGIIA H48Q to GBS NEM316
823 by fluorescence microscopy (+). As control, H48Q hGIIA mutant protein was omitted (-).
824 hGIIA was detected with a mouse anti-human hGIIA monoclonal antibody. An irrelevant
825 IgG1 isotype antibody served as negative control. The cell wall was labeled with Ester-350,
826 and newly formed septa were visualized with fluorescently labeled vancomycin (Vanc-FL),
827 which stains sites of peptidoglycan insertion. Shown are representative cells. Quantification
828 of hGIIA binding to polar or non-polar regions of GBS are based on analysis of 12 fields
829 including 578 stained cells from two separate experiments. For all other panels, data
830 represent mean +/- SD of three independent experiments.

831

832 **Fig S1. Endogenous hGIIA in normal human serum does not affect GAS growth.**
833 Addition of hGIIA inhibitor LY311727 does not influence GAS growth in human serum. Data
834 represent mean +/- SD of three independent experiments, ns = not significant.

835 **Fig S2. Biased transposon insertions in M5005_Spy_1390.** Unusual high number of
836 transposon insertions at one location in the gene M5005_Spy_1390.

837 **Fig S3. Tn-seq results.** Circos respresentation of the Tn-seq data. Each bar in the inner two
838 circles, where blue is control and red the hGIIA treated, represent the average RKPM value
839 of a gene. The following to circles represent the BH corrected *p*-value and the fold change in
840 log of the hGIIA treated samples vs control samples. Red bars indicate a fold a respective
841 fold decrease and green bars a respective fold increase of transposon insertions. The gene
842 highlighted in red is M5005_Spy_1390, which showed significant fold change due to unusual
843 high transposon insertions at one specific point in the gene.

844 **Fig S4. Three additional time points for $DiOC_2(3)$ measurements.** Membrane potential
845 after (A) 5 minutes, (B) 30 minutes and (C) 60 minutes of hGIIA stress. Data represent mean
846 +/- SD of three independent experiments. *, $p > 0.05$; **, $p > 0.01$; ***, $p > 0.001$.

847 **Fig S5. Kinetics of the SYTOX influx in intact GAS strains.** SYTOX influx measured over
848 120 minutes when GAS strains are incubated with (A) 5, (B) 0.5, (C) 0.1, (D) 0.01, (E) 0.001,
849 and (F) 0 µg/ml hGIIA. Data represent mean +/- SD of three independent experiments.

850 **Fig S6. Kinetics of the SYTOX influx in protoplast GAS strains.** SYTOX influx measured
851 over 120 minutes when protoplast GAS strains are incubated with (A) 5, (B) 0.5, (C) 0.1, (D)
852 0.01, (E) 0.001, and (F) 0 µg/ml hGIIA. Data represents mean +/- SD of three independent
853 experiments.

854

855 **Acknowledgements**
856 The authors would like to thank Dr. Michel-Yves Mistou (INRA, Jouy-en-Josas, France) for
857 providing his *gbcO* mutant and complemented GBS strains.

858 **Funding statement**

859 The funders had no role in study design, data collection and analysis, decision to publish, or
860 preparation of the manuscript. N.M.v.S and V.P.v.H were supported by a VIDI grant
861 (91713303) from the Dutch Scientific Organization (NWO).

Figure 1

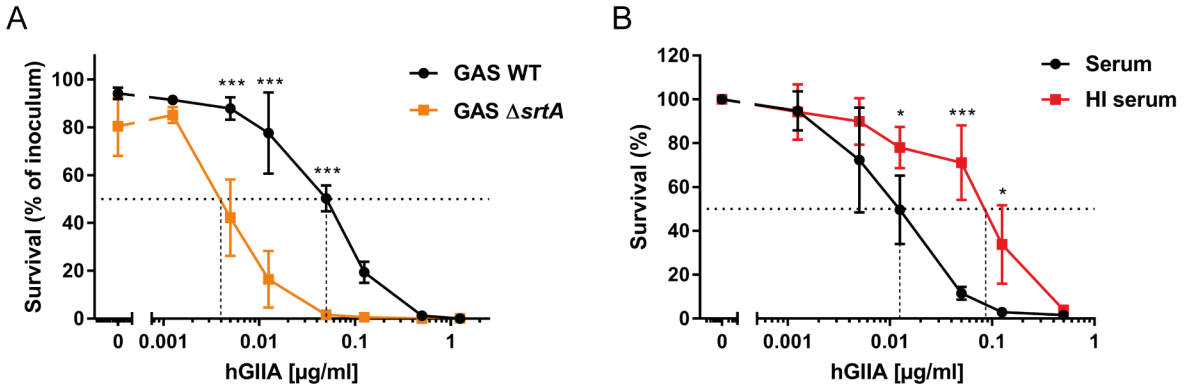
A
Survival (% of inoculum)
100
80
60
40
20
0
***
***
***
GAS WT
GAS Δ*srtA*
0
0.001
0.01
0.1
1
hGIIA [µg/ml]
B
Survival (%)
120
100
80
60
40
20
0
*
***
*
Serum
HI serum
0
0.001
0.01
0.1
1
hGIIA [µg/ml]

Figure 2

A

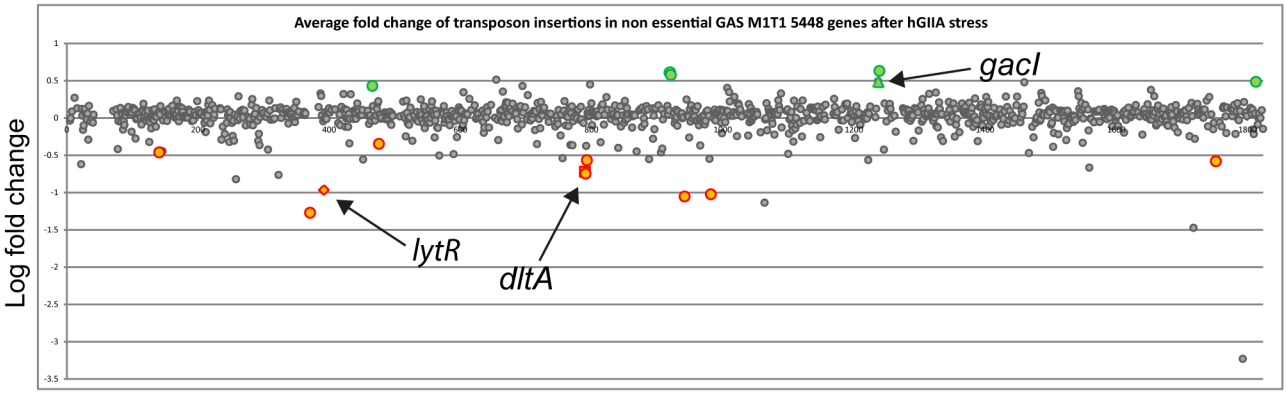
Average fold change of transposon insertions in non essential GAS M1T1 5448 genes after hGIIA stress
Log fold change
gacI
lytR
dltA

B

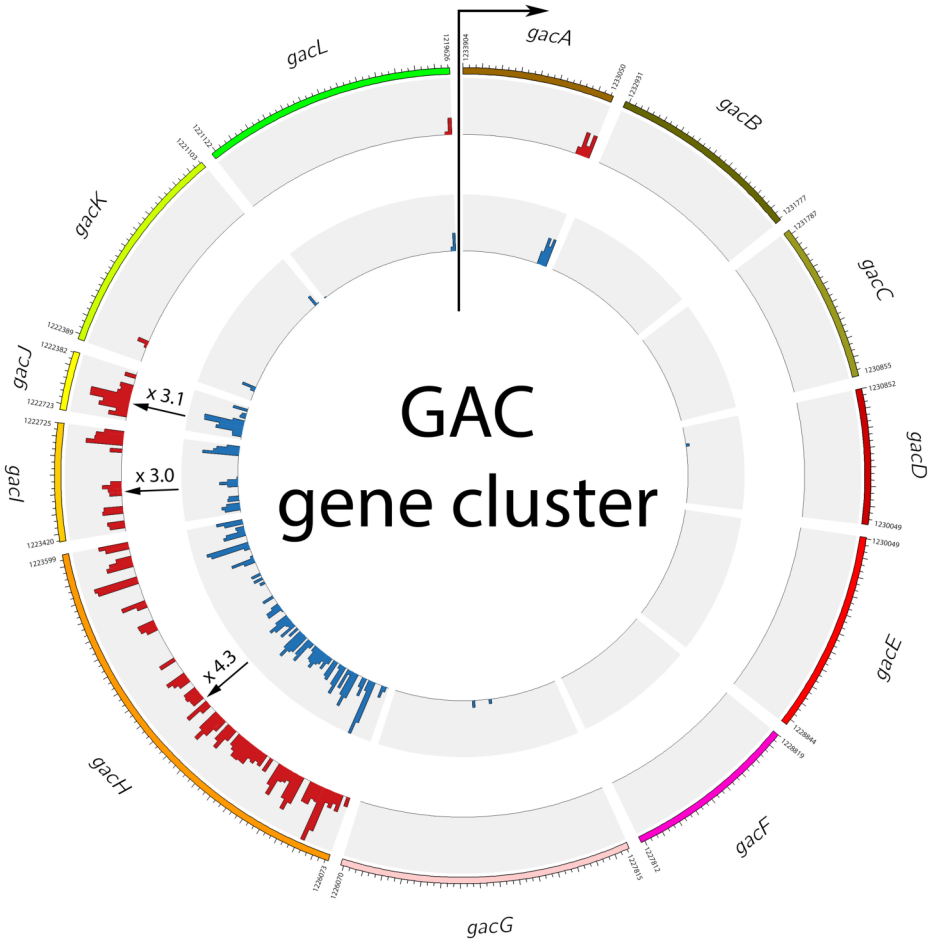
GAC
gene cluster
gacA
gacB
gacC
gacD
gacE
gacF
gacG
gacH
gacI
gacJ
gacK
gacL
x 3.1
x 3.0
x 4.3

Figure 3

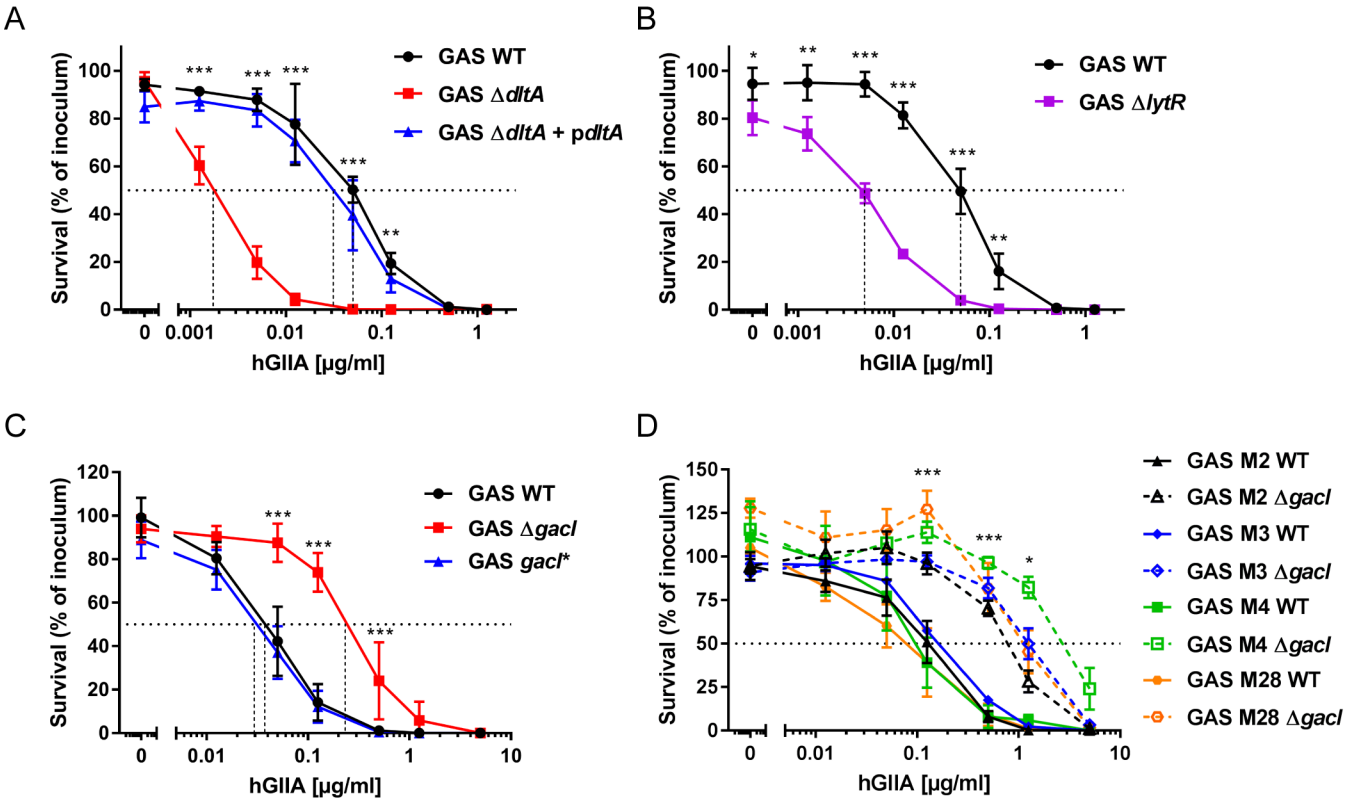
A
Survival (% of inoculum)
hGIIA [µg/ml]
GAS WT
GAS ΔdltA
GAS ΔdltA + pdltA
B
GAS WT
GAS ΔlytR
C
GAS WT
GAS ΔgacI
GAS gacI*
D
GAS M2 WT
GAS M2 ΔgacI
GAS M3 WT
GAS M3 ΔgacI
GAS M4 WT
GAS M4 ΔgacI
GAS M28 WT
GAS M28 ΔgacI

Figure 4

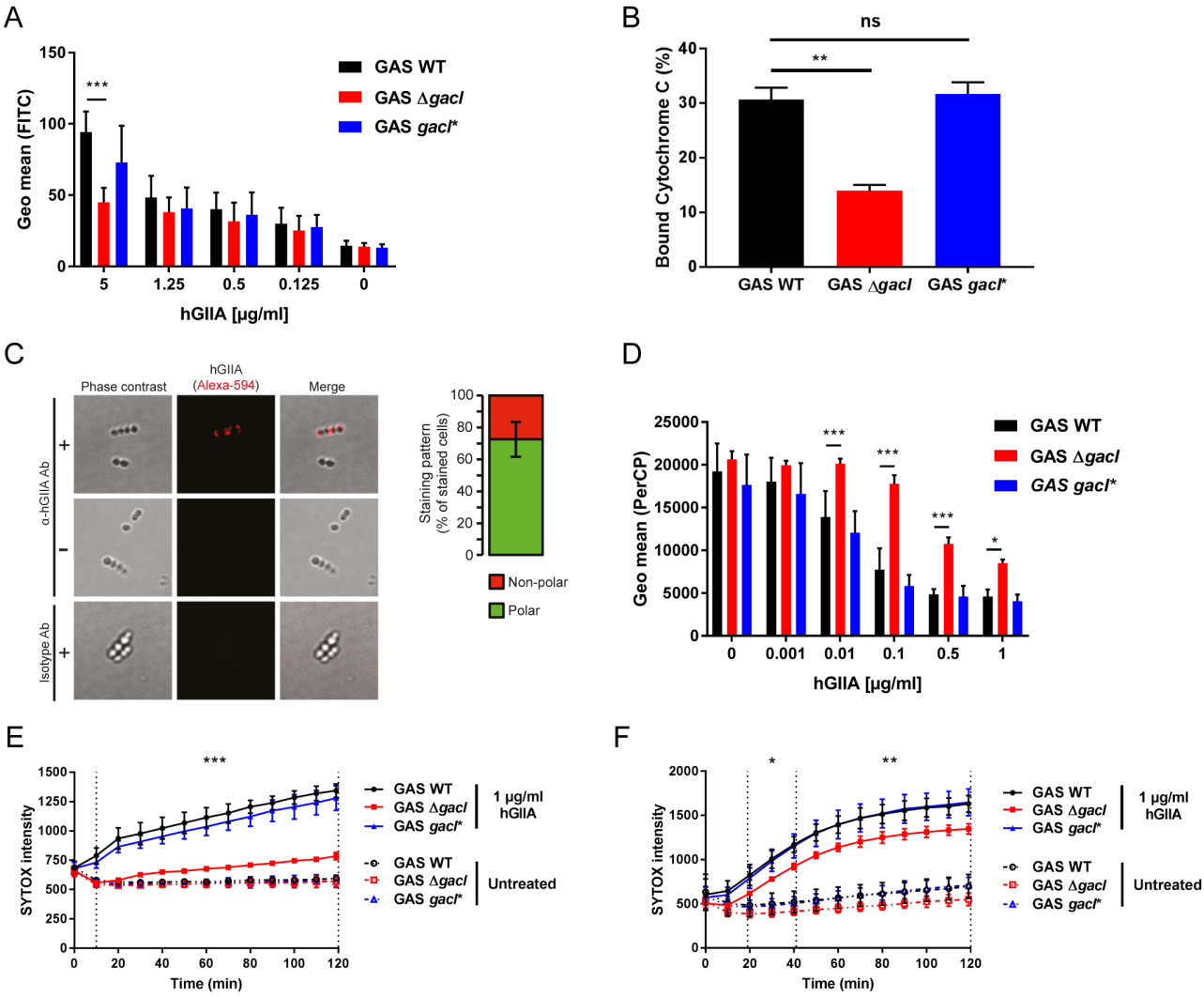
A
Geo mean (FITC)
150
100
50
0
***
GAS WT
GAS Δgacl
GAS gacl*
5
1.25
0.5
0.125
0
hGIIA [µg/ml]
B
ns
**
Bound Cytochrome C (%)
40
30
20
10
0
GAS WT
GAS Δgacl
GAS gacl*
C
Phase contrast
hGIIA
(Alexa-594)
Merge
α-hGIIA Ab
+
−
Isotype Ab
+
Staining pattern
(% of stained cells)
100
80
60
40
20
0
Non-polar
Polar
D
Geo mean (PerCP)
25000
20000
15000
10000
5000
0
***
***
***
*
GAS WT
GAS Δgacl
GAS gacl*
0
0.001
0.01
0.1
0.5
1
hGIIA [µg/ml]
E
SYTOX intensity
1500
1250
1000
750
500
250
0
***
GAS WT
GAS Δgacl
GAS gacl*
1 µg/ml
hGIIA
GAS WT
GAS Δgacl
GAS gacl*
Untreated
0
20
40
60
80
100
120
Time (min)
F
SYTOX intensity
2000
1500
1000
500
0
*
**
GAS WT
GAS Δgacl
GAS gacl*
1 µg/ml
hGIIA
GAS WT
GAS Δgacl
GAS gacl*
Untreated
0
20
40
60
80
100
120
Time (min)

Figure 5

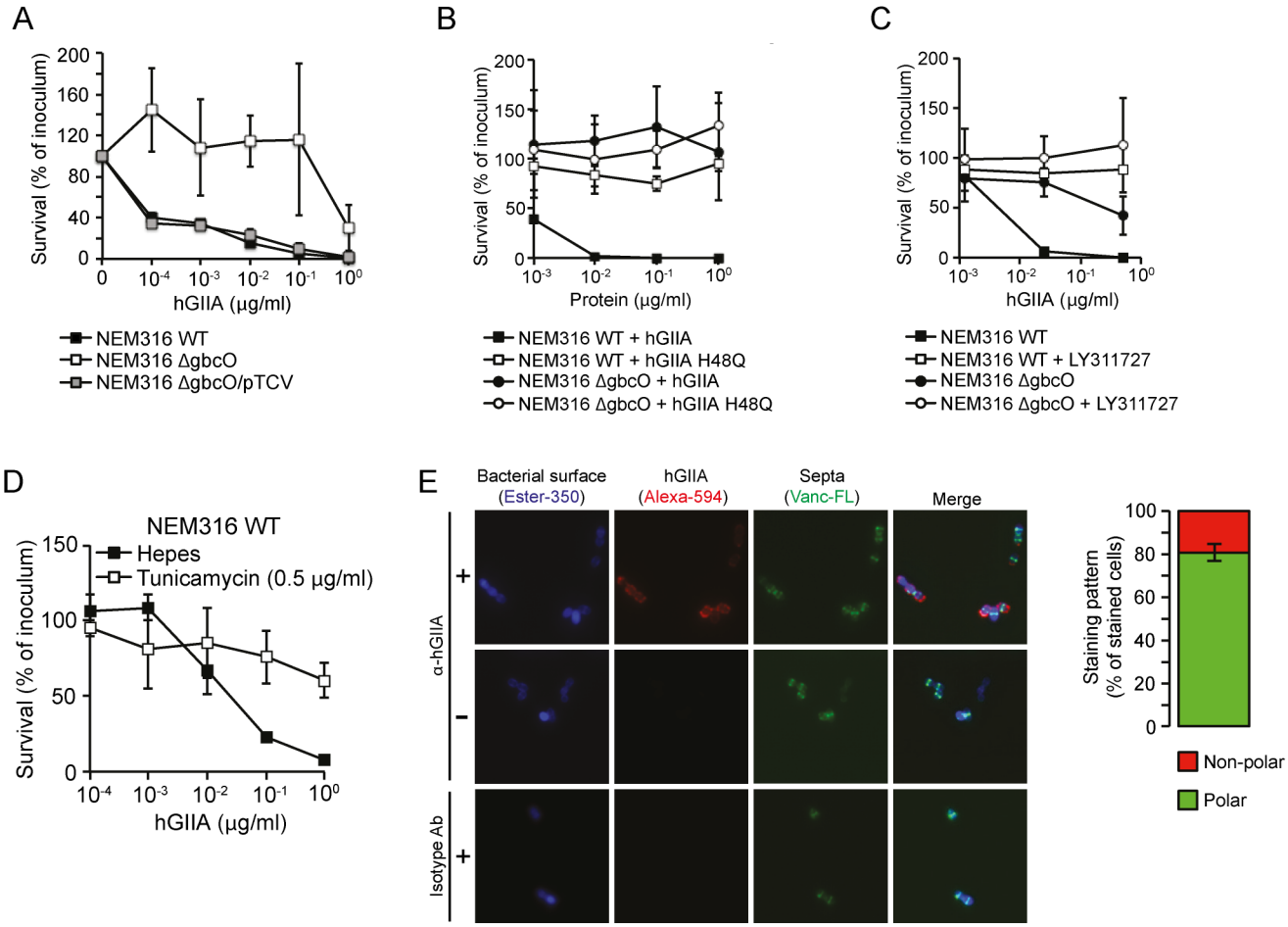
A
Survival (% of inoculum)
hGIIA (µg/ml)
NEM316 WT
NEM316 ΔgbcO
NEM316 ΔgbcO/pTCV
B
Survival (% of inoculum)
Protein (µg/ml)
NEM316 WT + hGIIA
NEM316 WT + hGIIA H48Q
NEM316 ΔgbcO + hGIIA
NEM316 ΔgbcO + hGIIA H48Q
C
Survival (% of inoculum)
hGIIA (µg/ml)
NEM316 WT
NEM316 WT + LY311727
NEM316 ΔgbcO
NEM316 ΔgbcO + LY311727
D
NEM316 WT
Hepes
Tunicamycin (0.5 µg/ml)
Survival (% of inoculum)
hGIIA (µg/ml)
E
Bacterial surface
(Ester-350)
hGIIA
(Alexa-594)
Septa
(Vanc-FL)
Merge
α-hGIIA
Isotype Ab
Staining pattern
(% of stained cells)
Non-polar
Polar